Optical Materials: X 24 (2024) 100378

Contents lists available at ScienceDirect

Optical Materials: X

journal homepage: www.journals.elsevier.com/optical-materials-x

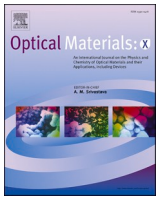

Invited Article

Optical and EPR study of Mn^{4+} ions in different crystal environments in Mn, Li co-doped MgO

L. Borkovska [a,*], K. Kozoriz [a], I. Vorona [a], O. Gudymenko [a], S. Ponomaryov [a], O. Melnichuk [b], V. Trachevskii [c], O. Chukova [d], L. Khomenkova [a]

[a] V. Lashkaryov Institute of Semiconductor Physics of NAS of Ukraine, 45 Pr. Nauky, Kyiv, 03028, Ukraine
[b] Mykola Gogol State University of Nizhyn, 2 Hrafska Str., Nizhyn, 16600, Ukraine
[c] Technical Center of NAS of Ukraine, 13 Pokrovs'ka Str., Kyiv, 04070, Ukraine
[d] Deutsches Elektronen-Synchrotron DESY, Notkestr. 85, Hamburg, 22607, Germany

ARTICLE INFO

Keywords:
MgO:Mn
Li co-doping
Mn^{4+} symmetry
Luminescence
EPR

ABSTRACT

The influence of Li ion on the symmetry of Mn^{4+} center and its photoluminescence (PL) in MgO:0,01%Mn, 3 % Li ceramics is studied by the X-ray diffraction, electron paramagnetic resonance (EPR), PL and optical absorption methods. It is shown that Li co-doping stimulates conversion of Mn^{2+} on Mg site into Mn^{4+} and can decrease symmetry of Mn^{4+} in a case of their specific close arrangement in the crystal lattice. Two kinds of Mn^{4+} centers are identified in the EPR and PL spectra: cubic Mn^{4+} and tetragonal complex Mn^{4+}-Li^{+}. The parameters of corresponding EPR centers are estimated from the experimental spectra ($g_{cub} = 1.994$, $|A|_{cub} = 70.9 \times 10^4$ cm^{-1}; $g_{1tetr} = g_{2tetr} = 1.994$, $g_{3tetr} = 1.993$, $|A|_{tetr} = 71 \times 10^4$ cm^{-1}, $|D|_{tetr} = 220 \times 10^4$ cm^{-1}). The PL lines observed in the low temperature PL spectra are assigned to the specific Mn^{4+} related centers using a complementary study of PL excitation spectra and temperature dependent PL spectra. The lines at 654 nm and 671 nm are ascribed to R-line of Mn^{4+} in a site of cubic symmetry and its phonon overtone, correspondingly, as well as the lines at 666 nm and 681 nm are attributed to R2 line of Mn^{4+} in site with tetragonal symmetry and to its phonon overtone, correspondingly. It is shown that in Mn doped MgO ceramics made without intentional Li co-doping, the cubic Mn^{4+} center can be present and contribute to the PL spectra.

1. Introduction

During the last decade, the interest to Mn^{4+} activated crystalline materials has been renewed due to the prospects of their use as the low-cost and environmental friendly red phosphors for application in blue-chip excited warm white light-emitting diodes, LEDs [1,2]. The red phosphors activated with Mn^{4+} are also considered for application in LEDs for indoor plant cultivation, thermometry, latent fingerprint visualization, temperature sensing, etc. [2–5]. The Mn^{4+} ion in octahedral crystal field exhibits relatively sharp emission lines (or several broad emission bands) in the 600–750 nm spectral range originating from $^2E \rightarrow {}^4A_2$ spin-forbidden transitions of Mn^{4+}. This emission can be excited via two broad absorption bands in the UV and blue-green spectral ranges caused by $^4A_2 \rightarrow {}^4T_1$ and $^4A_2 \rightarrow {}^4T_2$ spinallowed transitions of Mn^{4+} [2]. The splitting of the energy levels of Mn^{4+} free ion in a crystal field (CF) depends on the CF symmetry and strength, and in the ideal octahedral CF is described by the well-known Tanabe-Sugano diagram. In accordance with this diagram, the energy of the ^2E level is almost independent on CF strength. Instead, it is determined mainly by the nature of the surrounding ligands, namely, the covalence of the "Mn^{4+}- ligand" bonding. The more covalent chemical bonding results in smaller energy of the ^2E level. Since the length and angles between the chemical bonds determine an overlap between the Mn^{4+} ion and nearest-neighbor ligand anion, they also affect the energy of ^2E level [6].

Thermal stability of Mn^{4+} photoluminescence (PL) in certain host material is an important characteristic for its application as red phosphor. It has been proposed that thermal quenching of Mn^{4+} luminescence in different oxide and fluoride hosts occurs via thermally activated crossing of the $^4A_2$ ground level and the $^4T_2$ excited level [7]. This conclusion was made based on the correlation found between the

* Corresponding author.
E-mail addresses: l_borkovska@ukr.net (L. Borkovska), kozoriz.kostiantin@gmail.com (K. Kozoriz), ip_vorona@yahoo.com (I. Vorona), gudymen@ukr.net (O. Gudymenko), s.s.ponomaryov@gmail.com (S. Ponomaryov), mov310310@gmail.com (O. Melnichuk), trachev@imp.kiev.ua (V. Trachevskii), oksana.chukova@desy.de (O. Chukova), khomen@ukr.net (L. Khomenkova).

https://doi.org/10.1016/j.omx.2024.100378
Received 20 August 2024; Received in revised form 21 October 2024; Accepted 30 October 2024
Available online 6 November 2024

quenching temperature of Mn^{4+} luminescence, T½, (a temperature at which the intensity of Mn^{4+} emission decreases by a factor of 2) and the energy of $^4A_2 \rightarrow {}^4T_2$ transition, namely that the T½ increased with the energy of the $^4T_2$ level. The correlation suggests that in the hosts with larger CF strength, the Mn^{4+} PL should be observed up to higher temperatures.

In many Mn^{4+} activated red phosphors, co-doping strategy is applied. The concentration of co-dopants introduced for enhancement of Mn^{4+} PL intensity [8–14] varies in the range from single to several percent. If a co-dopant is located near Mn^{4+} ion, it can affect the PL of Mn^{4+} by changing the strength and symmetry of CF. It can influence the energy of the ^2E and $^4T_2$ levels as well as the kinetics of PL thermal quenching.

Co-doping with lithium is often used for enhancement of Mn^{4+} luminescence in different crystalline hosts since Li can act as charge compensator [8,11] as well as can decrease concentration of close Mn^{4+}-Mn^{4+} pairs [13] or other defects [12]. Besides, lithium salts, like LiCl, LiF, Li_2CO_3 and $LiNO_3$, used for Li co-doping, are the sintering additives which promote the diffusion of ions and enhance sintering mechanisms, facilitate crystal growth and affect crystal morphology [14–20]. In Mn-doped MgO, co-doping with Li, which substitutes Mg^{2+} site ion and acts as acceptor, $Li^{+}{}_{Mg}$, is used for conversion of Mn^{2+} on Mg^{2+} site to Mn^{4+} [21–23]. In this material, the effect of Li on the symmetry and luminescence of Mn^{4+} was found to be strongly pronounced. It has been suggested that the Mn^{4+} and Li^+ ions located side by side along the <100> direction form a complex Mn^{4+}-Li^+ with decreased symmetry, while the Mn^{4+} which has no Li at the nearest Mg^{2+} site remains in cubic symmetry. The Li^+ on Mg^{2+} site has an effective negative charge that causes an electrostatic interaction with neighbor O^{2-} ion resulted in the displacement of O^{2-} ions in the octahedron and the decrease of symmetry of Mn^{4+}-Li^{+} center to C_{4V}. In the electron paramagnetic resonance (EPR) spectra of Mn and Li co-doped MgO, the signals caused by Mn^{2+} as well as Mn^{4+} in cubic and tetragonal symmetry were clearly identified [22–25]. The calculated EPR parameters of the Mn^{4+}-Li^+ tetragonal center [25] agree reasonable with those estimated from the experimental spectra [22,24]. The low temperature PL spectra of Mn and Li co-doped MgO [21–23] showed several narrow bands in 650–680 nm spectral range. The lines at 653.4–654.5 nm, 663.4 and 666.09 nm demonstrated the highest intensity, and those at 659.8, 667.8 nm, as well as at 672.3 and 677.6 nm were much less intense. In Ref. [22], the 654.5 nm band was attributed to the R line of Mn^{4+} at a cubic symmetry site in MgO, and the other bands to its phonon overtones. At the same time, Nakada et al. [23] ascribed the most intense PL bands at 663.17 and 666.2 nm to R1 and R2 lines, i.e. electric dipole transitions in places with non-cubic symmetry. Thus, no clear correspondence between the individual lines observed in the PL spectra and the symmetry of the Mn^{4+} center was established.

In this work, the results of PL and EPR study of Mn related centers in Mn and Li co-doped MgO ceramics are presented. It is shown that complementary study of the PL excitation spectra of individual PL lines and temperature dependence of the PL spectra makes it possible to conclude about the cubic or tetragonal symmetry of Mn^{4+} center responsible for individual PL line.

2. Experimental details

The samples studied were the ceramics of MgO co-doped with 0.01 mol.% Mn and 3 mol.% Li as well as ceramics of MgO doped with 0.01 mol.% Mn only. The concentration of Li was chosen close to the value reported by other authors (about 5 mol.%) [21–23] for compensation of excess electric charge of Mn^{4+} in MgO, and the concentration of Mn was much lower to prevent concentration quenching of PL. Transmission electron microscopy study of raw MgO (98 %) powder (not shown here) revealed that it composed of the grains of strictly cubic shape with sizes varying from 50 to 200 nm and contained a small number of larger grains of sizes about several μm. Before the annealing the MgO powder was mixed thoroughly with corresponding amounts of $MnSO_4$ and $LiNO_3$ water solutions, dried at 100 °C and pressed into rectangular tablets with dimensions of (30–40) × 10 × 5 mm^3. The tablets were sintered in muffle furnace at 900, 1000, 1100 and 1200 °C for 3 h and cooled to room temperature during the natural cooling of the furnace.

The phase purity of the investigated MgO:Mn, Li ceramics was studied by X-ray diffraction (XRD) using $Cu_{K\alpha l}$ radiation ($\lambda = 0.15406$ nm) with operating voltage and current of 45 kV and 40 mA, respectively. The XRD patterns were collected in a symmetrical mode in the 2θ range of 10–110° (step 0.025°, exposition time 1.0 s per step) on a Philips X'Pert PRO - MRD diffractometer. EPR measurements were carried out at room temperature on X-band Bruker EPR ELEXSYS 580 spectrometer equipped with high-Q SHQE cavity using 100 kHz modulation of the magnetic field with amplitude of 1 G and the microwave power below 2 mW. All experimental EPR spectra were normalized on sample masses and Q factors of loaded cavity that allowed direct comparison of EPR signals in different samples (powders, ceramics). Simulation of EPR spectra was carried out using computer program "POWDER" from the "Visual EPR" software package developed and provided by Prof. V. Grachev as described in Ref. [26]. The PL and optical absorption spectra were detected using a BLACK-Comet C-SR-50 spectrometer and excited by the light of 411 nm continuous laser or xenon lamp, respectively. The PL excitation spectra were recalculated from the PL spectra recorded under excitation by light of different wavelengths obtained by passing the light of a xenon lamp through the monochromator. The PL excitation spectra were normalized to the same number of incident photons. The optical absorption spectra were studied at 293 K, the PL excitation spectra - at 77 K, and the PL spectra – at different temperatures in the range from 77 K to 293 K. The PL spectra were also measured at 9 K with a TIC-500 flow-type cryostat from CryoVac using synchrotron radiation excitation at the PETRA III P66 beamline of the Deutsches Elektronen-Synchrotron DESY (Hamburg, Germany). The PL spectra were excited at a wavelength of 160 nm, which corresponds to interband transitions in MgO. The spectra were registered with monochromator was a Kymera 328i (Andor) with F/4.1 aperture (200–1200 nm) and 0.4 nm spectral resolution and a Newton 920 CCD detector.

3. Results and discussion

Fig. 1 shows the Θ-2Θ scans of MgO:Mn, Li ceramics sintered at different temperatures. All the most intense diffraction peaks correspond to the polycrystalline phase of MgO (JCPDS No. 010-77-2364). In the XRD pattern of the sample annealed at 1200 °C, the peaks of low intensity at 2Θ ~ 52.34° and 2Θ ~ 65.24° appear. Most likely, these peaks are due to some secondary phase composed of lithium, aluminium (coming from ceramic tube used as a sample holder in a furnace) and magnesium oxide. Lattice parameters of MgO phase determined by Rietveld refinement using the High Score Plus program as well as the size of the coherent scattering region and the average deformation determined by the Williamson-Hall method are shown in Table 1. In the last case, the half-widths of (200) reflex (2Θ = 42.94°) and (400) reflex (2Θ = 94.11°) were analyzed.

As the annealing temperature increases to 1100 °C, the deformations of the crystal lattice increase and the size of coherent scattering region decreases slightly. These can be an evidence of the generation of defects apparently due to increased doping of the MgO phase. However, at 1200 °C, the size of the coherent scattering region increases slightly and the average deformations decrease. The latter can be a signature of decreased doping, for instance, due to Li evaporation or the formation of some secondary phase.

The EPR spectrum of the ceramics co-doped with Mn and Li and sintered at 900 °C (Fig. 2) shows three sharp multicomponent signals with *g*-factor of about 2.0 which match well those caused by Mn^{2+} and Mn^{4+} ions in cubic and tetragonal symmetry in the MgO [22–24]. The single line with g~1.98 was ascribed to the EPR signal caused by Cr^{3+}

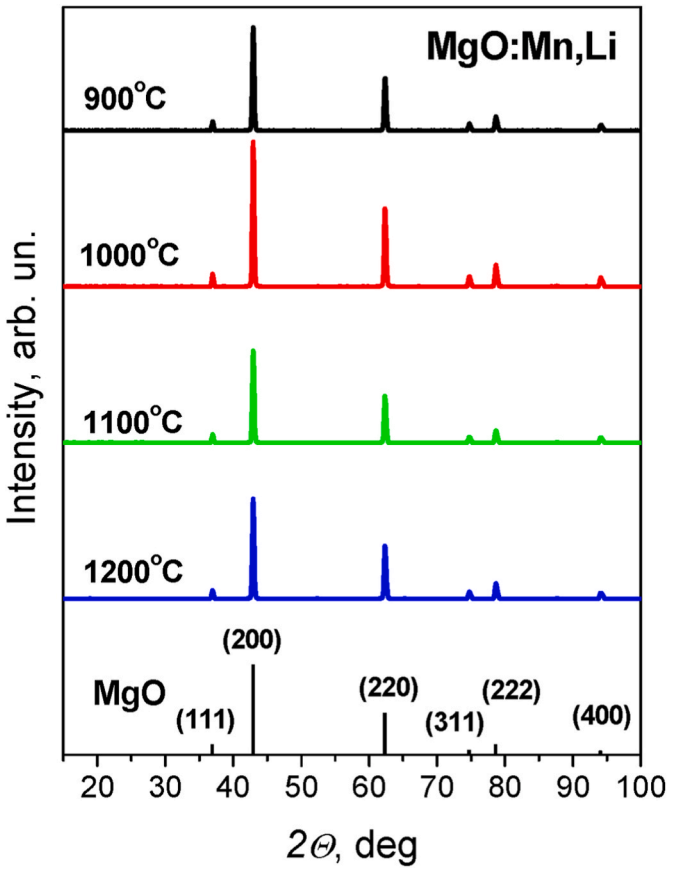

Fig. 1. XRD spectra of MgO:Mn,Li ceramics sintered at different temperatures.

Table 1
The parameters of MgO crystal phase in MgO:Mn, Li ceramics obtained from the analysis of XRD patterns.

Annealing temperature, °C	Lattice parameter, Å	Average deformations, %	Size of coherent scattering region, nm
900	4.2109	0.048	28.4
1000	4.2108	0.072	26.3
1100	4.2108	0.083	25.6
1200	4.2103	0.065	27.1

residual impurity. The experimental spectrum was simulated by the sum of these four signals using the spin Hamiltonian containing the electron and nuclear Zeeman interactions, as well as the hyperfine and fine interactions:

$$H = g\beta\mathbf{BS} - g_N\beta_N\mathbf{BI} + \boldsymbol{A}\mathbf{SI} + \sum_{n,m} f_n b_n^m O_n^m \quad (1)$$

where $\boldsymbol{g}$ and $\boldsymbol{A}$ – tensors of spectroscopic splitting and hyperfine interaction, **S** and **I** – electron and nuclear spin operators, β – Bohr magneton, g_N – nuclear g-factor, β_N – nuclear magneton, f_n – multipliers, b_n^m – fine structure parameters, O_n^m – extended Stevens operators.

The parameters of the observed paramagnetic centers of manganese obtained from the simulation of the experimental spectrum are in good agreement with the parameters reported by other authors [22–25] for Mn^{2+} and Mn^{4+} ions at octahedral and tetrahedral sites of MgO co-doped with Mn and Li (Table 2).

In the EPR spectra of the ceramics made without Li (Fig. 3b), the same signals are found except of tetragonal Mn^{4+}-Li^{+} center. Moreover, the signal due to cubic Mn^{4+} is of low intensity and can be resolved only for the ceramics sintered at 900 and 1000 °C (Fig. 3b–d). In the case of

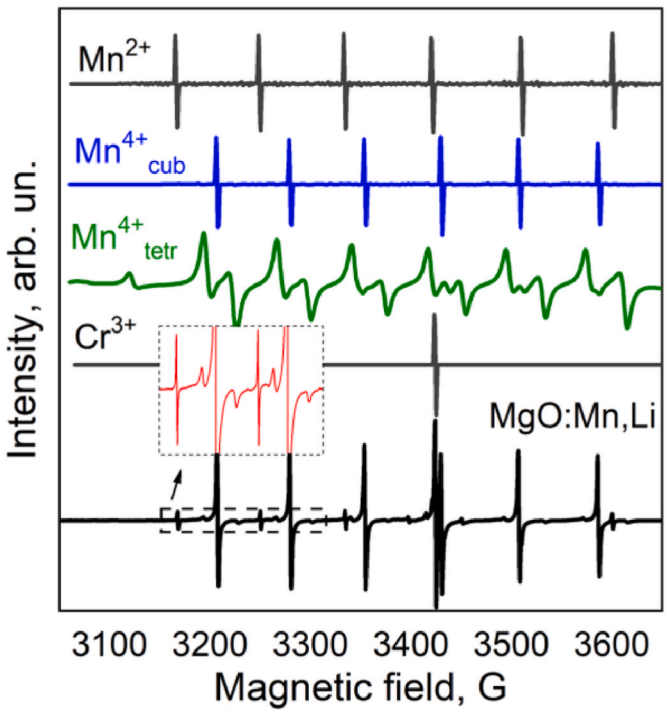

Fig. 2. Experimental EPR spectrum of MgO:0.01%Mn, 3%Li ceramics sintered at 900 °C and simulated EPR spectra of Cr^{3+}, Mn^{2+}, cubic Mn^{4+} and tetragonal Mn^{4+}-Li^{+} centers in MgO. The insert shows an enlarged part of experimental spectrum outlined by a dashed line.

the absence of intentional Li co-doping, the compensation of excess electric charge of Mn^{4+} on Mg^{2+} site can be carried out either by residual impurity ions of lithium, sodium, etc. [27,28], or by magnesium vacancies [29].

The intensity of the revealed EPR signals varies with the annealing temperature (Fig. 3e and f). As the annealing temperature increases to 1100 °C, the intensity of Mn^{2+} signal starts increasing and that of Mn^{4+} decreases. In the EPR spectra of Li co-doped ceramics sintered at 1200 °C, the signal of cubic Mn^{4+} can still be distinguished (Fig. 3c), but it decreases in intensity by more than 10 times, and the intensity of Mn^{2+} signal increases in several times as compared with the sample annealed at 1000 °C (Fig. 3a). In the ceramics made without Li, the intensity of Mn^{2+} signal increases at high annealing temperatures too (Fig. 3b). This means that the concentration of manganese substituted Mg^{2+} sites increases with annealing temperature. Therefore, the decrease of Mn^{4+} EPR signal at 1200 °C in Li co-doped ceramics is not caused by the decrease of the amount of manganese ions on Mg sites, but is the result of the reduction of Mn^{4+} to Mn^{2+} apparently due to the decrease of concentration of charge compensating defects acting as acceptors. The latter can have several reasons. Firstly, since the alkali impurities tend to leave the oxide at temperatures beyond 800 K [30], an intense evaporation of Li is expected at high annealing temperatures [31] as well as Li can gather on the dislocation lines and agglomerate into tiny Li–O units [30]. Secondly, it is possible that at high temperatures more Li occupies an interstitial position in MgO lattice and acts as a donor or Li^{+}_{Mg} form neutral or charged complexes with adjacent an O vacancy which acts as a donor [30]. More research is needed to find out the exact cause. Whatever the reason, Li co-doping of MgO ceramics is efficient for the oxidation of Mn^{2+} to Mn^{4+} at temperatures not exceeding 1100 °C.

The presence of Li^{+} acceptors also affects the concentration of Cr^{3+} centers since Cr^{3+}_{Mg} needs charge compensation too. In fact, the EPR signal of Cr^{3+} is about twice larger in Li co-doped ceramics. However, it increases in intensity with annealing temperature in contrast to the EPR signal of Mn^{4+} (Fig. 3e and f).

Table 2
Paramagnetic resonance parameters of the Mn^{2+}, cubic Mn^{4+} and tetragonal Mn^{4+}- Li^{+} centers in MgO.

Reference	Mn^{2+} in MgO		Mn^{4+}_{cub} in MgO		Mn^{4+}_{tetr} in MgO	
	g	$\|A\| \times 10^4$ cm^{-1}	g	$\|A\| \times 10^4$ cm^{-1}	g_1, g_2, g_3	$\|A\| \times 10^4$, cm^{-1} $\|D\| \times 10^4$, cm^{-1}
This work MgO:Mn, Li	**2.0016**	**81.5**	**1.994**	**70.9**	**$g_1=g_2=1.994$ $g_3=1.9931$**	**A=71 D=220**
Nakada [23], MgO:Mn, Li	2.0014 ±0.0005	81.0 ±0.2	1.99 ±0.002	72 ±0.4	–	–
Rubio [24], MgO:Mn, Li	–	–	1.9937(3)	71.02(5)	$g_\perp = 1.9941(3)$; $g_\parallel = 1.9937(3)$;	$A_\perp = 70.98(5)$; $A_\parallel = 71.02(5)$; D = 234.9(6)
Henderson [22] MgO:Mn, Li	–	–	1. 9948 ±0.0003	70.0	1. 995 ±0.001	A = 70.8 D = 280
Wu [25] (calculations) MgO:Mn, Li	–	–	–	–	$g_\perp = 1.9938$; $g_\parallel = 1.9936$;	D = 234

In the optical absorption spectra of all Mn-doped ceramics (Fig. 4), a broad band peaked at about 515–520 nm is observed. The intensity of this band is higher in Li co-doped samples as well as in those sintered at 900–1000 °C. As the annealing temperature exceeds 1000 °C, the intensity of this absorption decreases.

The low-temperature PL spectra of Li co-doped samples show the series of PL lines in the red spectral region (Fig. 5a) which agree well with those reported for spin-forbidden $^2E \rightarrow {}^4A_2$ transitions of the Mn^{4+} (the bands in the range of 650–695 nm) and Cr^{3+} (in the range of 695–750 nm) on Mg site in the MgO [21–23]. The intensity of Mn^{4+} emission is the largest in the ceramics sintered at 900 °C and 1000 °C and decreases noticeably as the annealing temperature increases to 1200 °C. This is consistent with the decrease in intensity of the EPR signals caused by Mn^{4+} centers at high annealing temperatures. In the PL spectra of the ceramics made without Li (Fig. 5b), strongly overlapped PL bands are found in the same spectral regions. The intensity of Mn^{4+} emission is more than 10 times smaller than in Li co-doped samples in agreement with much lower intensity of Mn^{4+} EPR signal (Fig. 3). The intensity of Cr^{3+} emission is nearly the same in the ceramics sintered at 1200 °C with and without Li confirming that Cr is a residual impurity.

Comparison of the low-temperature PL spectra of the ceramics made with and without Li co-doping reveals the differences that do not depend on how the excitation of luminescence occurs, i.e., through the *d-d* transitions of Mn^{4+} (Fig. 6a) or through the interband transitions of MgO (Fig. 6b). Specifically, the PL spectra of the samples made without Li co-doping demonstrate strongly overlapped PL bands with the most intense one peaked at 671 nm. In contrast, in the PL spectra of Li co-doped ceramics the individual PL bands at about 654, 666, 671 and 681 nm are well resolved and the intensity of the line at 666 nm is much larger or comparable to that of the band at 671 nm.

The interpretation of different PL bands can be made based on the analysis of both PL excitation spectra and temperature dependence of PL spectra. The study of low-temperature PL spectra excited with light of different wavelengths (Fig. 7a) reveals strong variation in the relative intensities of different PL lines. Specifically, the lines at 654 nm and 671 nm are well pronounced under 410 nm excitation and almost disappear under 550 nm excitation. At the same time, the lines at 666 nm and 681 nm are observed in the PL spectra under excitation with light of 410 nm, 490 nm and 550 nm. The excitation spectra of the 654 nm and 666 nm PL lines (Fig. 7b) show the band peaked at about 470 nm. This excitation band can be ascribed to spin-allowed $^4A_2 \rightarrow {}^4T_2$ transition of the Mn^{4+} in MgO. The long wavelength edge of this band is stretched to 540 nm for the 654 nm PL line and to about 600 nm for the 666 nm PL line. In the last case, the excitation band has a shoulder at about 515–520 nm. It can be supposed that this is the peak of the excitation band for the 666 nm PL line. The presence of intense peak at 470 nm can be explained by the possible contribution of the 671 nm PL line to the excitation spectrum of the 666 nm PL line. It should be noted that the same absorption band with flat maximum stretched from 450 to 520 nm is found in the optical absorption spectra (Fig. 4). Similar absorption band centered at 520 nm has been already reported for Mn-doped MgO crystals [32]. This band was ascribed to $5E \rightarrow 5T_2$ spin-allowed transition of Mn^{3+} substituted Mg site ions. We cannot exclude that optical transitions of Mn^{3+} also contribute to the absorption in the 450–650 spectral range especially in the ceramics made without Li co-doping.

The red shift of the absorption edge of the PL excitation band implies the decrease in the energy of $^4A_2 \rightarrow {}^4T_2$ transition. This means the decrease of CF strength that can be a consequence of the decrease of symmetry of the environment for the Mn^{4+} ions. Similarly, a strong red shift of the PL excitation bands caused by $^4A_2 \rightarrow {}^4T_1$ and $^4A_2 \rightarrow {}^4T_2$ transitions has been observed for Cr^{3+} ions in the rhombohedral position in the MgO [33]. Therefore, the PL lines at 654 nm and 671 nm can be attributed to the electronic transitions of the Mn^{4+} in the site of cubic symmetry, and the lines at 666 nm and 681 nm are related to Mn^{4+} in the site of tetragonal symmetry.

This assignment of PL lines receives additional confirmation from the analysis of temperature dependence of the PL spectra (Fig. 8a). In Li co-doped ceramics, all above mentioned Mn^{4+} PL lines show strong thermal quenching with temperature increase starting from about 170 K. Thermal quenching of PL lines at 654 and 671 nm starts at higher temperatures than of the lines at 666 and 681 nm (Fig. 8*b and c*). Specifically, the temperature at which the PL intensity decreases by a factor of two, $T_{1/2}$, is about 215 K for the 671 nm line and about 190 K for the 666 nm PL line. Similarly, the difference in temperature dependence of PL intensity has been reported for the PL lines of Cr^{3+} in cubic and tetragonal sites in MgO [33,34]. The obtained results agree well with an explanation of Mn^{4+} PL thermal quenching proposed in Ref. [7]. The statement that the $T_{1/2}$ increases with the energy of the $^4A_2 \rightarrow {}^4T_2$ transition is also true for the Mn^{4+} centers in different crystal environments in MgO.

In the PL spectrum of Li co-doped ceramics recorded at 9 K, a line at 654 nm demonstrates the shortest wavelength spectral position (Fig. 6b). The line with a close spectral position (653.3–654.5 nm) was observed in the low-temperature emission spectra of Mn-doped MgO by different authors [21,22,27,35]. In case no Mn^{4+} emission at shorter wavelengths was found, this band was ascribed to the zero-phonon line (R-line) of the transition of the Mn^{4+} ion in near-octahedral symmetry [27]. However, in Ref. [35] this band was ascribed to the electronic transition of Mn^{4+} occupying non-octahedral symmetry sites because of a weak PL line at ~651.9 nm which was assigned to the R-line of Mn^{4+} in the site of near-octahedral symmetry [27,35]. Our results allow attributing the line at 654 nm to the R-line of Mn^{4+} in the site of cubic symmetry and the most intense line at 666 nm to the R2 line of Mn^{4+} in the site with tetragonal symmetry. The bands at 671 and 681 nm are the phonon overtones of corresponding emissions. The interpretation of the R2 line is consistent with that proposed in Ref. [23]. We also cannot exclude that the band at about 663 nm ascribed in Ref. [23] to R1 line of Mn^{4+} in a place with non-cubic symmetry is also present in our PL spectra (Fig. 6) being hardly resolved.

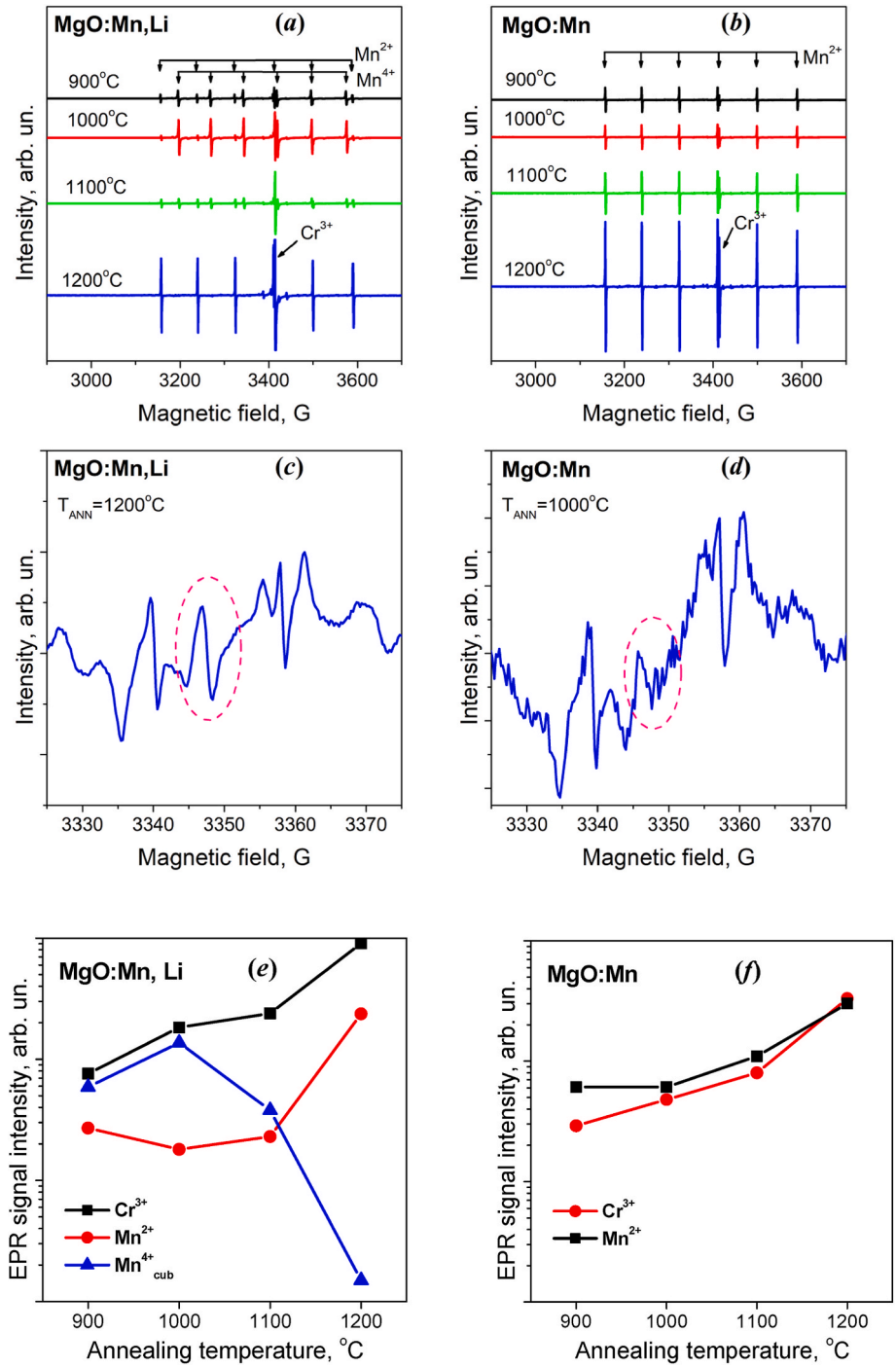

Fig. 3. EPR spectra of MgO:0.01%Mn,3%Li (*a*) and MgO:0.01%Mn (*b*) ceramics sintered at different temperatures, and the enlarged part of EPR spectra of Li co-doped MgO:Mn ceramics sintered at 1200 °C (*c*) and MgO:Mn ceramics sintered at 1000 °C (*d*); relative contribution of Mn^{2+}, Mn^{4+}, and Cr^{3+} paramagnetic centers versus annealing temperature extracted from EPR signals of MgO:Mn, Li (*e*) and MgO–Mn (*f*) ceramics. T = 293 K.

In the low temperature PL spectrum MgO:Mn ceramics made without Li co-doping, only the line at 671 nm is resolved (Fig. 6b) and the PL bands due to tetrahedral Mn^{4+}-Li complexes are not visible. This is not surprising due to low concentration of charge compensating defects acting as acceptors.

It should be noted that as the temperature increases, the additional PL lines at ~637 nm and ~644 nm arise and their relative contribution to the PL spectra increases (Fig. 8*a*). These lines can be ascribed to anti-Stokes phonon modes of Mn^{4+} transition in near-octahedral environment in MgO [36].

4. Conclusions

The EPR spectra, PL, PL excitation and optical absorption spectra of 0.01 % manganese doped MgO ceramics sintered with and without Li co-doping (3 %) at different temperatures in the range of 900–1200 °C are investigated. It is shown that Li co-doping is efficient for charge compensation of Mn^{4+} on the Mg site only in the ceramics sintered at temperatures not higher than 1100 °C. The EPR signals due to Mn^{2+}, Mn^{4+} in the cubic environment and tetrahedral Mn^{4+}-Li^{+} complex are detected and their parameters are identified. In the low temperature PL spectra of Li co-doped ceramics, the lines at about 654, 666, 671 and

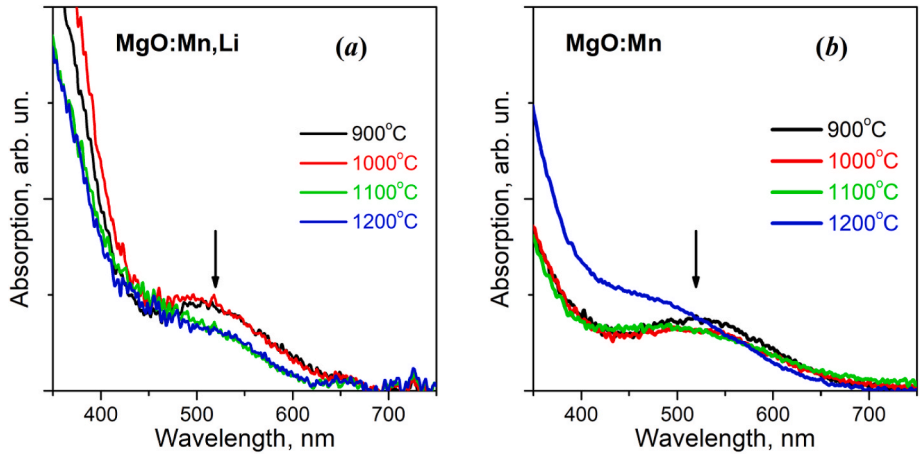

Fig. 4. Optical absorption spectra of MgO:Mn,Li (*a*) and MgO:Mn (b) ceramics sintered at different temperatures. T = 293 K.

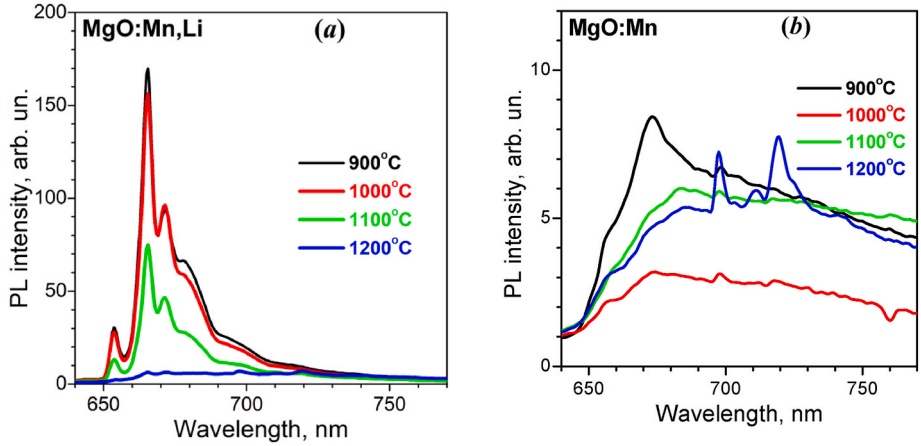

Fig. 5. Low-temperature PL spectra of Li co-doped MgO:Mn ceramics (*a*) and MgO:Mn ceramics (*b*) sintered at different temperatures. T = 77 K, λ_{EXC} = 410 nm.

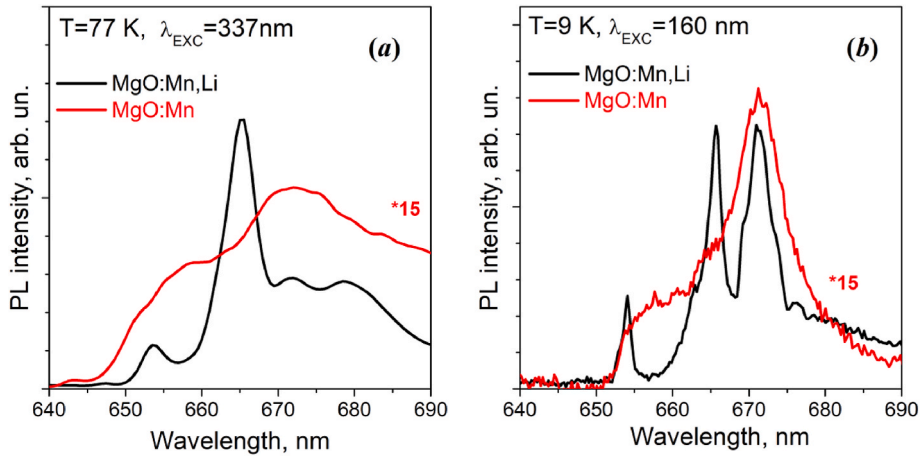

Fig. 6. The PL spectra of MgO:Mn and MgO:Mn,Li ceramics sintered at 1000 °C and recorded under excitation with light of 337 nm at 77 K (*a*) and with light of 160 nm at 9 K (*b*).

681 nm related to Mn^{4+} emission are detected. The lines at 654 nm and 666 nm are ascribed to the R-line of Mn^{4+} in the site of cubic symmetry and the R2 line of Mn^{4+} in the site with tetragonal symmetry, correspondingly, and the bands at 671 and 681 nm to phonon overtones of corresponding emissions. In the excitation spectra Mn^{4+} PL lines, the band peaked at about 470 nm is observed and ascribed to $^4A_2 \rightarrow {}^4T_2$ transition of Mn^{4+} in cubic environment. A shoulder at about 520 nm found in the excitation spectra of 666 and 681 nm lines is attributed to $^4A_2 \rightarrow {}^4T_2$ transition of Mn^{4+} in site with tetragonal symmetry. It is shown that thermal quenching of PL intensity of the lines at 654 and 671 nm starts at higher temperatures than of the lines at 666 and 681 nm in agreement with the higher energy of $^4A_2 \rightarrow {}^4T_2$ transition. It is shown that

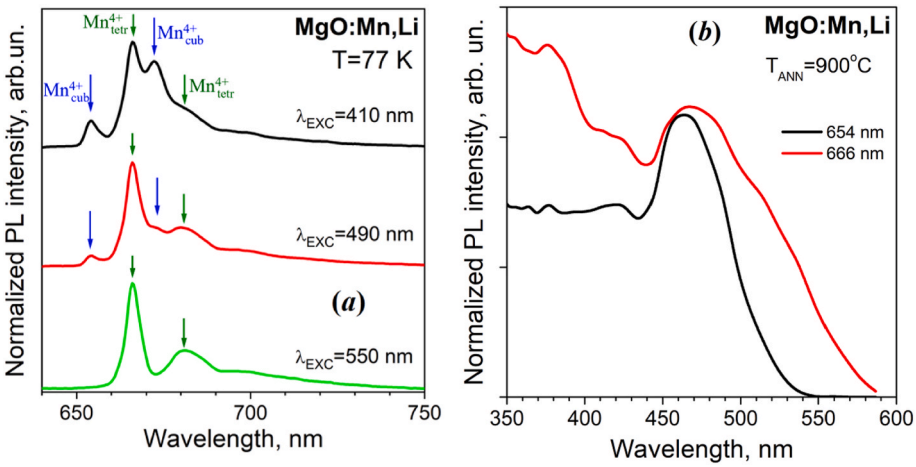

Fig. 7. Low temperature PL spectra of Li co-doped MgO:Mn ceramics (T_{ANN} = 900 °C) under different excitations (*a*) and PL excitation spectra of 654 nm and 666 nm lines of MgO:Mn,Li ceramics sintered at 1000 °C (*c*), T = 77 K.

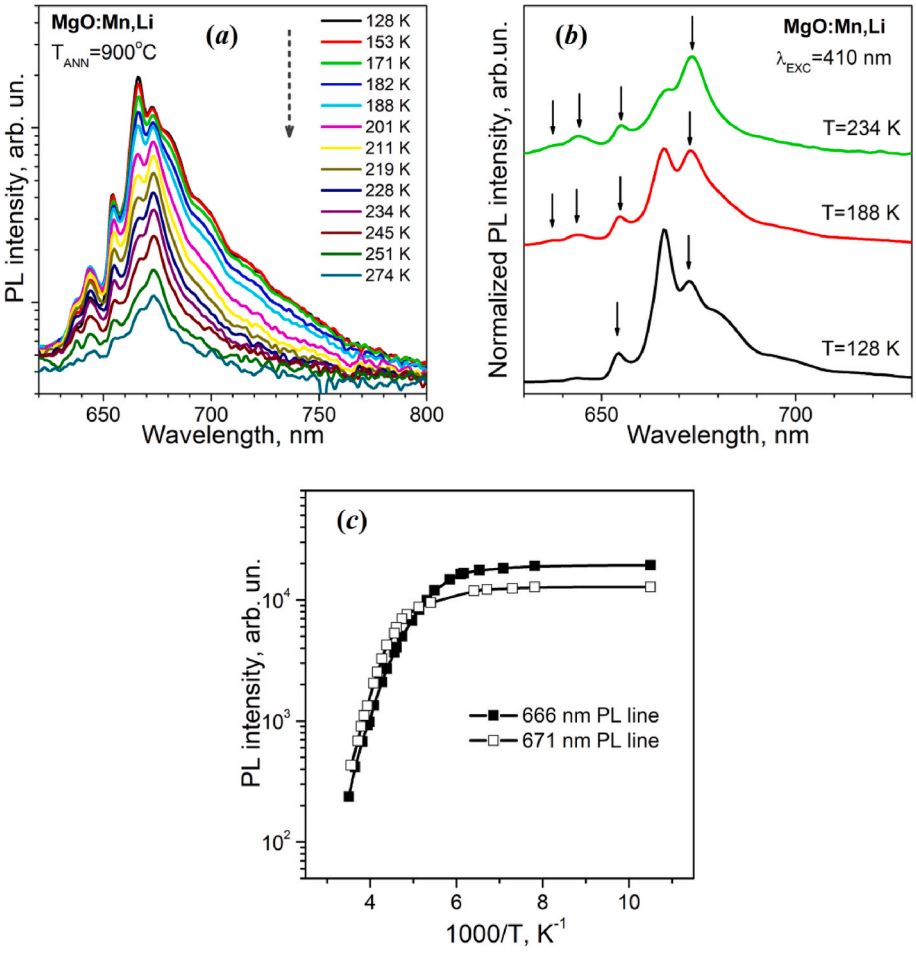

Fig. 8. Temperature dependencies of the PL spectra (*a,b*) and PL intensity of 666 nm and 671 nm lines (*c*) of MgO:Mn,Li ceramics sintered at 900 °C, λ_{EXC} = 410 nm.

in the EPR and PL spectra of the ceramics made without Li co-doping the signals due to Mn^{4+} ions in cubic environment are also present.

CRediT authorship contribution statement

L. Borkovska: Writing – review & editing, Writing – original draft, Visualization, Validation, Supervision, Investigation, Formal analysis, Conceptualization. **K. Kozoriz:** Writing – review & editing, Visualization, Investigation, Data curation. **I. Vorona:** Writing – review & editing, Validation, Investigation, Formal analysis, Data curation. **O. Gudymenko:** Investigation, Validation, Writing – review & editing. **S. Ponomaryov:** Writing – review & editing, Resources, Formal analysis, Data curation. **O. Melnichuk:** Writing – review & editing, Validation, Funding acquisition. **V. Trachevskii:** Writing – review & editing, Validation, Resources, Data curation. **O. Chukova:** Writing – review & editing, Validation, Investigation. **L. Khomenkova:** Writing – review &

editing, Visualization, Validation, Investigation.

Declaration of competing interest

The authors declare that they have no known competing financial interests or personal relationships that could have appeared to influence the work reported in this paper.

Acknowledgments

This work was supported by the National Academy of Sciences of Ukraine as well as by the National Research Foundation of Ukraine from the state budget, project 2020.02/0380 «Structure transformation and non-equilibrium electron processes in wide bandgap metal oxides and their solid solutions». The authors acknowledge also DESY (Hamburg, Germany) for the provision of experimental facilities at PETRA III Beamline P66 (proposal I-20231041 EC) as well as DESY User Office for financial support from the NEPHEWS project which is funded by the HORIZON-Europe program.

Data availability

Data will be made available on request.

References

[1] Q. Zhou, L. Dolgov, A.M. Srivastava, L. Zhou, Z. Wang, J. Shi, M.D. Dramićanin, M. G. Brik, M. Wu, Mn^{2+} and Mn^{4+} red phosphors: synthesis, luminescence and applications in WLEDs, A review, Journal of Materials Chemistry C 6 (2018) 2652–2671, https://doi.org/10.1039/c8tc00251g.

[2] S. Adachi, Review - Mn^{4+}-activated red and deep red-emitting phosphors, ECS Journal of Solid State Science and Technology 9 (2019) 016001, https://doi.org/10.1149/2.0022001jss.

[3] Z. Wang, H. Lin, D. Zhang, Y. Shen, Y. Li, R. Hong, C. Tao, Z. Han, L. Chen, S. Zhou, Deep-red emitting Mg_2TiO_4:Mn^{4+} phosphor ceramics for plant lighting, Journal of Advanced Ceramics 10 (2020) 88–97, https://doi.org/10.1007/s40145-020-0421-6.

[4] E. Glais, V. Đorđević, J. Papan, B. Viana, M.D. Dramićanin, $MgTiO_3$:Mn^{4+} a multi-reading temperature nanoprobe, RSC Adv. 8 (2018) 18341–18346, https://doi.org/10.1039/c8ra02482k.

[5] S.-H. Yang, Y.-C. Hung, P.-C. Tseng, H.-Y. Lee, Versatile deep-red Mg_2TiO_4:Mn^{4+} phosphor for photoluminescence, thermometry, and latent fingerprint visualization, J. Alloys Compd. 801 (2019) 394–401, https://doi.org/10.1016/j.jallcom.2019.06.028.

[6] M.G. Brik, S.J. Camardello, A.M. Srivastava, Influence of covalency on the Mn^{4+} $2E_G \rightarrow {}^4A_{2g}$ Emission energy in crystals, ECS Journal of Solid State Science and Technology 4 (2014) R39–R43, https://doi.org/10.1149/2.0031503jss.

[7] T. Senden, R.J.A. Van Dijk-Moes, A. Meijerink, Quenching of the red Mn^{4+} luminescence in Mn^{4+}-doped fluoride LED phosphors, Light Sci. Appl. 7 (2018), https://doi.org/10.1038/s41377-018-0013-1.

[8] T. Jansen, J. Gorobez, M. Kirm, M.G. Brik, S. Vielhauer, M. Oja, N.M. Khaidukov, V.N. Makhov, T. Jüstel, Narrow band deep red photoluminescence of $Y_2Mg_3Ge_3O_{12}$:Mn^{4+}, Li^+ Inverse garnet for high power phosphor converted LEDs, ECS Journal of Solid State Science and Technology 7 (2017) R3086–R3092, https://doi.org/10.1149/2.0121801jss.

[9] R. Cao, J. Huang, X. Ceng, Z. Luo, W. Ruan, Q. Hu, $LiGaTiO_4$:Mn^{4+} red phosphor: synthesis, luminescence properties and emission enhancement by Mg^{2+} and Al^{3+} ions, Ceram. Int. 42 (2016) 13296–13300, https://doi.org/10.1016/j.ceramint.2016.05.138.

[10] T. Murata, T. Tanoue, M. Iwasaki, K. Morinaga, T. Hase, Fluorescence properties of Mn^{4+} in $CaAl_{12}O_{19}$ compounds as red-emitting phosphor for white LED, J. Lumin. 114 (2005) 207–212, https://doi.org/10.1016/j.jlumin.2005.01.003.

[11] Z. Qiu, T. Luo, J. Zhang, W. Zhou, L. Yu, S. Lian, Effectively enhancing blue excitation of red phosphor Mg_2TiO_4:Mn^{4+} by Bi^{3+} sensitization, J. Lumin. 158 (2015) 130–135, https://doi.org/10.1016/j.jlumin.2014.09.032.

[12] M. Han, H. Tang, L. Liu, Y. Wang, X. Zhang, L. Lv, Tuning the Mn^{4+} coordination environment in Mg_2TiO_4 through a codoping strategy for enhancing luminescence performance, J. Phys. Chem. C 125 (2021) 15687–15695, https://doi.org/10.1021/acs.jpcc.1c04293.

[13] Y.X. Pan, G.K. Liu, Influence of Mg^{2+} on luminescence efficiency and charge compensating mechanism in phosphor $CaAl_{12}O_{19}$:Mn^{4+}, J. Lumin. 131 (2011) 465–468, https://doi.org/10.1016/j.jlumin.2010.11.014.

[14] L. Borkovska, L. Khomenkova, I. Markevich, M. Osipyonok, T. Stara, O. Gudymenko, V. Kladko, M. Baran, S. Lavoryk, X. Portier, T. Kryshtab, Effect of Li^+ co-doping on structural and luminescence properties of Mn^{4+} activated magnesium titanate films, J. Mater. Sci.: Mat. Electron. 29 (2018) 15613–15620, https://doi.org/10.1007/s10854-018-9153-6.

[15] M. Valant, D. Suvorov, R.C. Pullar, K. Sarma, N.McN. Alford, A mechanism for low-temperature sintering, J. Eur. Ceram. Soc. 26 (2006) 2777–2783, https://doi.org/10.1016/j.jeurceramsoc.2005.06.026.

[16] L. Khomenkova, V.I. Kushnirenko, M.M. Osipyonok, O.F. Syngaivsky, T. V. Zashivailo, G.S. Pekar, YuO. Polishchuk, V.P. Kladko, L.V. Borkovska, Structural, electrical and luminescent properties of ZnO:Li films fabricated by screen-printing method on sapphire substrate, Phys. Status Solidi C 12 (2015) 1144–1147, https://doi.org/10.1002/pssc.201400232.

[17] J. Chen, C. Li, Z. Hui, Y. Liu, Mechanisms of Li^+ ions in the emission enhancement of $KMg_4(PO_4)_3$:Eu^{2+} for white light emitting diodes, Inorg. Chem. 56 (2017) 1144–1151, https://doi.org/10.1021/acs.inorgchem.6b02140.

[18] J. Zhou, Y. Wang, B. Liu, J. Liu, Photoluminescence properties of $BaMgAl_{10}O_{17}$:Eu^{2+} phosphor prepared by the flux method, J. Phys. Chem. Sol. 72 (2011) 995–1001, https://doi.org/10.1016/j.jpcs.2010.08.017.

[19] A. Lacanilao, G. Wallez, L. Mazerolles, V. Buissette, T. Le Mercier, F. Aurissergues, M.-F. Trichet, N. Dupré, B. Pavageau, L. Servant, B. Viana, A structural approach of the flux effect on blue phosphor BAM:Eu ($BaMgAl_{10}O_{17}$:Eu^{2+}), Mat. Res. Bull. 48 (2013) 2960–2968, https://doi.org/10.1016/j.materresbull.2013.04.044.

[20] D. Kim, K.-W. Jeon, J.S. Jin, S.-G. Kang, D.-K. Seo, J.-C. Park, Remarkable flux effect of Li-codoping on highly enhanced luminescence of orthosilicate Ba_2SiO_4:Eu^{2+} phosphors for NUV-LEDs: autonomous impurity purification by eutectic Li_2CO_3 melts, RSC Adv. 5 (2015) 105339–105346, https://doi.org/10.1039/c5ra19712k.

[21] J.S. Prener, A magnesium oxide phosphor activated by tetravalent manganese, J. Chem. Phys. 21 (1953) 160–161, https://doi.org/10.1063/1.1698572.

[22] B. Henderson, T.P.P. Hall, Some studies of Cr^{3+} ions and Mn^{4+} ions in magnesium oxide, Proc. Phys. Soc. 90 (1967) 511–518. http://iopscience.iop.org/0370-1328/90/2/322.

[23] M. Nakada, K. Awazu, S. Ibuki, Electron spin resonance of Mn^{4+} ion MgO, J. Phys. Soc. Japan 19 (1964) 781, https://doi.org/10.1143/JPSJ.19.781.

[24] J. Rubio, Y. Chen, M.M. Abraham, Tetravalent manganese in lithium doped MgO and CaO, J. Chem. Phys. 64 (1976) 4804–4806, https://doi.org/10.1063/1.432039.

[25] X.-X. Wu, W. Fang, W.-L. Feng, W.-C. Zheng, Study of EPR parameters and defect structure for two tetragonal impurity centers in MgO:Cr^{3+} and MgO:Mn^{4+} crystals, Appl. Magn. Reson. 35 (2009) 503–510, https://doi.org/10.1007/s00723-009-0181-5.

[26] V. Nosenko, I. Vorona, V. Grachev, S. Ishchenko, N. Baran, Y. Becherikov, A. Zhuk, Y. Polishchuk, V. Kladko, A. Selishchev, The crystal structure of micro- and nanopowders of ZnS studied by EPR of Mn^{2+} and XRD, Nanoscale Res. Lett. 11 (2016) 517, https://doi.org/10.1186/s11671-016-1739-4.

[27] A.M. Glass, T.M. Searle, Reactions between vacancies and impurities in magnesium oxide. II. Mn^{4+} ion and OH^- ion impurities, J. Chem. Phys. 4646 (1967) 2092–2101, https://doi.org/10.1063/1.1841005.

[28] H. Suzuka, S. Hasegawa, T. Tanaka, G. Zhang, H. Hattori, Reversible change in the valence state of manganese ions between tetravalent and divalent states on a sodium-mounted magnesium oxide surface, Surf. Sci. Lett. 221 (1989) L769–L773, https://doi.org/10.1016/0167-2584(89)90640-3.

[29] J.J. Davies, S.R. Smith, J.E. Wertz, Electron paramagnetic resonance of tetravalent manganese ions at tetragonal and octahedral sites in MgO, Phys. Rev. 178 (1969) 608–612, https://doi.org/10.1103/PhysRev.178.608.

[30] N.A. Richter, F. Stavale, S.V. Levchenko, N. Nilius, H.-J. Freund, M. Scheffler, Defect complexes in Li-doped MgO, Phys. Rev. B 91 (2015) 195305, https://doi.org/10.1103/PhysRevB.91.195305.

[31] A.M. Glass, Reactions between vacancies and impurities in magnesium oxide. I. Cr^{3+}Ion impurities, J. Chem. Phys. 46 (1967) 2080–2091, https://doi.org/10.1063/1.1841004.

[32] P. Koidl, K.W. Blazey, Optical absorption of MgO:Mn, J. Phys. C Solid State Phys. 9 (1976) L167–L170, https://doi.org/10.1088/0022-3719/9/6/008.

[33] F. Castelli, L.S. Forster, Fluorescence ($^4T_2 \rightarrow {}^4A_2$) and phosphorescence ($^2E \rightarrow {}^4A_2$) in MgO:$Cr^{3+}$, Phys. Rev. B 11 (1975) 920–928, https://doi.org/10.1103/PhysRevB.11.920.

[34] M.O. Henry, J.P. Larkin, G.F. Imbusch, Nature of the broadband luminescence center in MgO:Cr^{3+}, Phys. Rev. B 13 (1976) 1893–1902, https://doi.org/10.1103/PhysRevB.13.1893.

[35] K. Dunphy, W.W. Duley, Multiphonon excitation of Mn^{4+} and Cr^{3+} luminescence in MgO, J. Phys. Chem. Solids 51 (1990) 1077–1082, https://doi.org/10.1016/0022-3697(90)90067-P.

[36] S. Adachi, Photoluminescence properties of Mn^{4+}-activated oxide phosphors for use in white-LED applications: a review, J. Lumin. 202 (2018) 263–281, https://doi.org/10.1016/j.jlumin.2018.05.053.